LAWRENCE
LIVERMORE
NATIONAL
LABORATORY

LLNL-PROC-483374

Geothermal Energy Production from Actively-Managed CO2 Storage in Saline Formations

T. A. Buscheck, Y. Sun, Y. Hao, M. Chen, B. Court, M. A. Celia, W. L. Bourcier, T. J. Wolery

May 9, 2011

Geothermal Resources Council 35th Annual Meeting
San Diego, CA, United States
October 23, 2011 through October 26, 2011

Disclaimer

Geothermal Energy Production from Actively-Managed CO_2 Storage in Saline Formations

Thomas A. Buscheck[a], Yunwei Sun[a], Yue Hao[a], Mingjie Chen[a], Benjamin Court[b], Michael A. Celia[b], William L. Bourcier[a], and Thomas J. Wolery[a]

[a]Lawrence Livermore National Laboratory, Livermore, CA USA
[b]Department of Civil and Environmental Engineering, Princeton University, Princeton, NJ USA

Keywords: CO_2 capture and sequestration (CCS), sedimentary formations, binary-cycle geothermal, injectivity, horizontal wells

Abstract

Increased reliance on geothermal energy and CO_2 capture and sequestration (CCS) in deep geological formations are both regarded as a promising means of lowering the amount of CO_2 emitted to the atmosphere and thereby mitigate climate change. We investigate an approach to produce geothermal energy and to sequester CO_2 at low cost and risk by integrating geothermal production with CCS in saline, sedimentary formations where a significant portion of the U.S. geothermal resource base resides. For industrial-scale CO_2 injection in saline formations, pressure increase can be a limiting factor in storage capacity and security, while geothermal energy production can be limited by pressure depletion. Our approach utilizes Active CO_2 Reservoir Management, which combines brine production with CO_2 injection to enable more cost-effective and secure CO_2 storage. The complementary CCS and geothermal systems are integrated synergistically, with CO_2 injection providing pressure support to maintain productivity of geothermal wells, while brine production provides pressure relief and improved injectivity for CO_2 injectors. A volumetric balance between injected and produced fluids mitigates the environmental and economic risks of reservoir overpressure (CCS concern) or underpressure (geothermal concern), including induced seismicity, insufficient well productivity or injectivity, subsidence, and fluid leakage either to or from overlying formations. We investigate the tradeoff between pressure relief at CO_2 injectors and CO_2 breakthrough time at geothermal brine producers for both vertical and horizontal wells, and address the influence of formation dip and permeability heterogeneity. The combined influence of buoyancy and layered heterogeneity delays CO_2 breakthrough at geothermal production wells, particularly when the permeability contrast is large. Our results indicate adequate pressure relief at CO_2 injectors can be attained, while delaying CO_2 breakthrough at production wells for 30 or more years, thus enabling sustainable geothermal power.

1. Introduction

Increased reliance on renewable energy sources, such as geothermal, as well as CO_2 capture and sequestration (CCS) in deep geological formations are both regarded as a promising means of lowering the amount of CO_2 emitted to the atmosphere and thereby mitigate global climate change. We investigate an approach to produce geothermal energy and to sequester CO_2 at low cost and risk by integrating geothermal energy production with CCS in saline, sedimentary formations. A significant portion of the U.S. geothermal resource base resides in sedimentary formations (MIT 2006). Much of this resource base exists in locations, such as the Midwest, where the need also exists to reduce CO_2 emissions and where the cost of electricity is relatively high (Buscheck, 2010). Lawrence Livermore National Laboratory (Buscheck et al., 2011a,

2011b, 2011c; Aines et al., 2011) and Princeton University (Court et al., 2011a, 2011b), are developing an approach, called Active CO_2 Reservoir Management (ACRM), which combines CO_2 injection, brine production and desalination, and residual-brine reinjection to produce fresh water, and, if formation temperatures are high enough, geothermal energy (Buscheck, 2010). Besides fresh-water production, ACRM can also enable other beneficial utilization options for the produced brine, such as water for cooling purposes, the extraction of mineral commodities, and make-up water for reservoir pressure support in oil, gas, and geothermal energy production (Buscheck et al., 2011b, 2011c; Harto and Veil, 2011; Bourcier et al., 2007, 2011).

For industrial-scale CO_2 injection in saline formations, pressure increase can be a limiting factor in storage capacity and is the main physical drive for potential CO_2 and brine leakage out of the storage formation (Birkholzer and Zhou, 2010). On the other hand, depending on reservoir size and continuity, geothermal energy production can be limited by pressure depletion. These two complementary systems can be integrated synergistically (Fig. 1), with CO_2 injection providing pressure support to maintain the productivity of geothermal wells, while the production of geothermal brine provides pressure relief and improved injectivity for CO_2 injectors. An integrated geothermal–CCS system, actively managed to yield a volumetric balance between injected and produced fluids, mitigates the environmental and economic risks of reservoir overpressure (CCS concern) or underpressure (geothermal concern), including induced seismicity, insufficient well productivity or injectivity, subsidence, and fluid leakage either to or from overlying formations, with minimal impacts on potable-water aquifers, including the issues of water depletion and contamination (Buscheck, 2010).

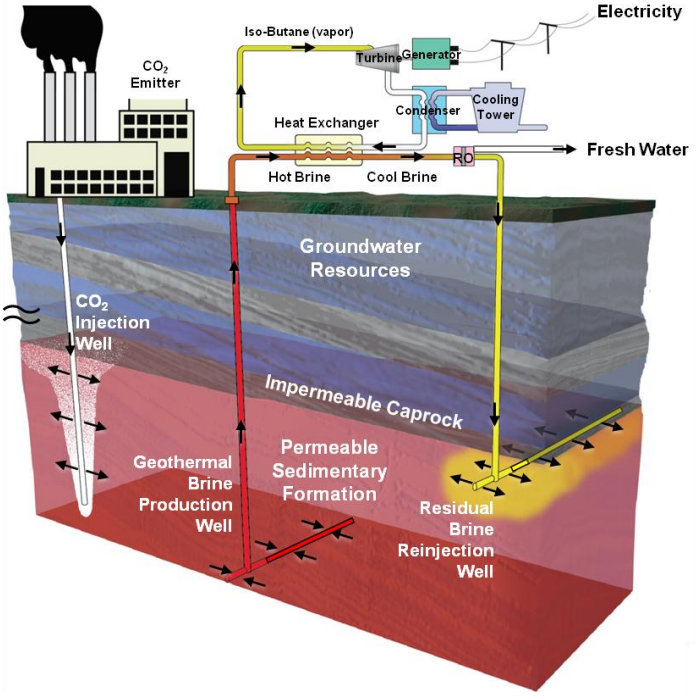

Fig. 1. An actively managed, integrated geothermal-CCS reservoir system is shown in a saline, sedimentary formation. Hot brine is produced from the formation, put through a binary-cycle geothermal plant where it is cooled and put through RO treatment to produce fresh water. Residual brine is reinjected into the same formation. This is an example of single-formation ACRM (Fig. 2b).

Preliminary economic analyses (Neal et al., 2011) indicate the possibility that brine production and reverse osmosis (RO) desalination can reduce CCS storage costs, and produced fresh water (Aines et al., 2011) can satisfy the increased water demand from CO_2 capture operations (Court et al., 2011a). Therefore, for economic and environmental reasons, the brine-production infrastructure may be included in many CCS systems, leaving only the surface-facility costs to be amortized for geothermal energy production. In addition, the process of CCS permitting will generate reservoir data that will be useful for conducting geothermal feasibility analyses. For ACRM, it is important to delay CO_2 breakthrough because produced CO_2 can be corrosive and reduce CO_2-storage efficiency. Therefore, optimized, cost-effective ACRM requires CO_2 injectors and brine producers being spaced and operated to achieve sufficient pressure interference, while delaying the breakthrough of injected CO_2 or reinjected residual brine to geothermal production wells, which will assure sustainable power production. Because our approach is designed to only produce native fluids, rather than injected CO_2, we can utilize conventional geothermal-power plant facilities. The leveraging of the brine-production infrastructure will reduce the levelized cost of electricity, and together with sustainable power production, will reduce financial risks for the geothermal energy producer.

The determination of the feasibility of deploying actively managed integrated geothermal-CCS at a given site depends on several primary factors (Buscheck, 2010) (Fig. 2a), including:

- **Formation CO_2-trapping characteristics:** (1) storage-formation volume, permeability, porosity, and depth and (2) caprock "seal" thickness, areal extent, and permeability.
- **Proximity to industrial-scale CO_2 emitters:** affecting CO_2-conveyance costs via pipelines.
- **Formation temperature:** affecting energy production rate per unit mass of produced brine.
- **Adequate brine disposition options:** (1) RO desalination and (2) saltwater cooling towers are options that reduce the volume of residual brine requiring reinjection; and (3) make-up water for reservoir pressure support in oil, gas, and geothermal energy production (Fig. 3b), which is an option that can be deployed in tandem with options 1 and 2, depends on the proximity to the oil, gas, or geothermal reservoir.

Ideally, all of these attributes would be co-located within a single CO_2 storage formation, which we call *single-formation* ACRM (Fig. 2b). However, it may be possible to deploy ACRM using separate formations in "tandem", with one formation being utilized for CO_2 storage and a separate formation being utilized for the purpose of brine reinjection (Fig. 3a). *Tandem-formation* ACRM involves two or more formations that posses less than all of the attributes listed above (Buscheck, 2010). For example, a formation with excellent CO_2 storage/trapping characteristics and good proximity to CO_2 emitters could be used in tandem with a formation with marginal CO_2 storage/trapping characteristics and low-salinity brine that could be treated at relatively low cost. Brine produced from the first (CO_2-storage) formation would be conveyed (via pipeline) and injected into the second (brine-storage) formation. If temperatures are high enough, brine produced from either formation could be used for binary-cycle geothermal energy production. Another form of tandem-formation ACRM involves conveying the produced brine to a geothermal reservoir (Fig. 3b), either a conventional hydrothermal or enhanced geothermal system (EGS), where it would be used as make-up water, or, in the case of EGS, the working fluid itself (Harto and Veil, 2011; Bourcier et al., 2007, 2011; Buscheck et al., 2011b, 2011c).

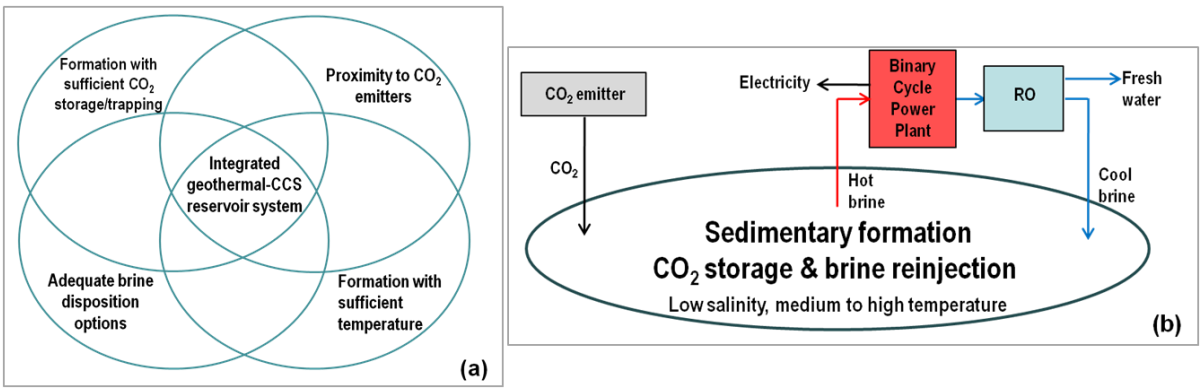

Fig. 2. (a) Venn diagram of attributes used to determine deployment potential for an integrated geothermal-CCS reservoir system. (b) Schematic of *single-formation* ACRM integrated with binary-cycle geothermal power and RO fresh water production.

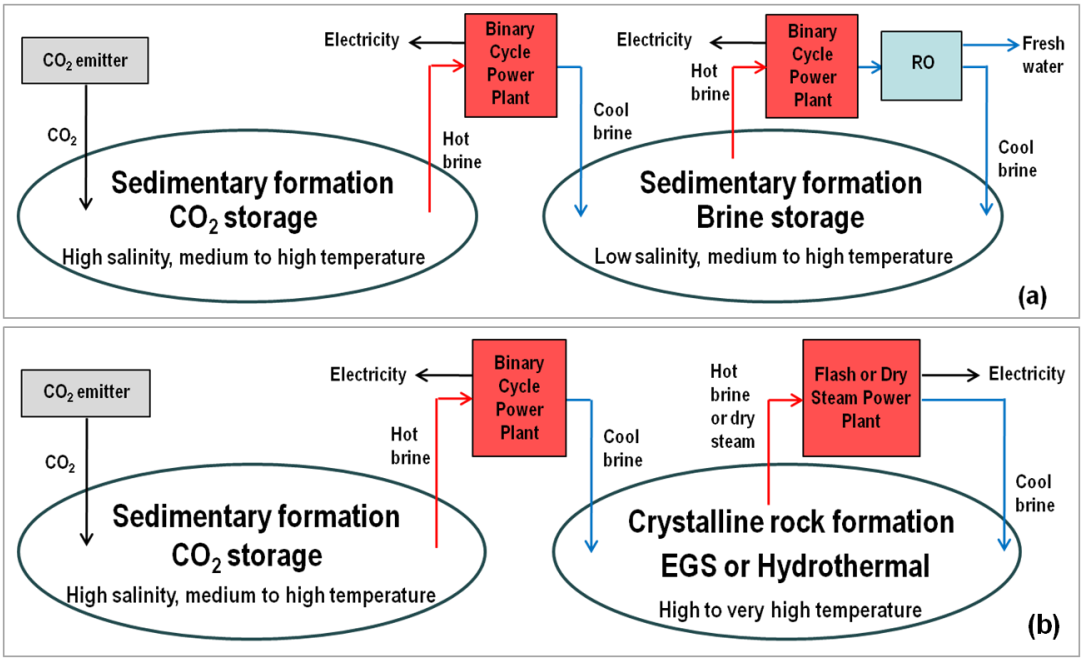

Fig. 3. (a) Schematic of *tandem-formation* ACRM integrated with binary-cycle geothermal power from both reservoirs and RO fresh water production from the brine-storage reservoir and (b) *tandem-formation* ACRM with binary-cycle geothermal power from the CO_2 storage reservoir and either flash or dry steam geothermal power from the brine-storage reservoir in crystalline rock.

Large geothermal well flow rates are possible with ACRM associated with a coal-fired power plant. If the produced volume of brine is equal to the injected CO_2 volume (extraction ratio = 1), and the ratio of produced fresh water to RO-treated brine is 0.5, and the residual brine is reinjected into the same formation, a brine-production rate of 760 kg/s is required for the volume of CO_2 to be sequestered for a 1-GWe pulverized-coal-fired power plant (Buscheck, 2010). If the residual brine is reinjected into a separate formation, a brine-extraction rate of 380 kg/sec is required for the same volume of CO_2. The left y axis of Fig. 4 is applicable to binary-cycle geothermal power output when it is integrated with ACRM for a 1-GWe pulverized-coal-fired power plant for an extraction ratio of 1.0 and no residual-brine reinjection in the CO_2 storage

formation. The right y axis in Fig. 4 is applicable when the ratio of produced fresh water to RO-treated brine is 0.5 and the residual brine is reinjected into the same formation (Fig. 2b). For a formation temperature of 120°C, which is achievable in potential CCS sites such as the Rock Springs Uplift in Wyoming (Surdam et al., 2009), an extraction ratio of 1.0, and an exit temperature of 25°C, binary-cycle geothermal could generate ~60 MWe for the CO_2 emitted by the nearby 2.2 GWe Jim Bridger coal-fired power plant, if single-formation ACRM (Fig. 2b) were used, with a fresh water-to-RO-treated-brine ratio of 0.5. If the residual brine were reinjected in a geothermal reservoir as make-up water (Fig. 3b), ~30 MWe could be generated in the first formation. If tandem-formation ACRM (Fig. 3a) were used, binary-cycle geothermal could generate ~90 MWe. If that tandem-formation ACRM case was scaled up to sequester all CO_2 emitted by coal-fired electricity generated in the State of Wyoming (6.2 GWe), this could generate ~254 MWe and produce 60,275 acre-feet of fresh water (Buscheck, 2010).

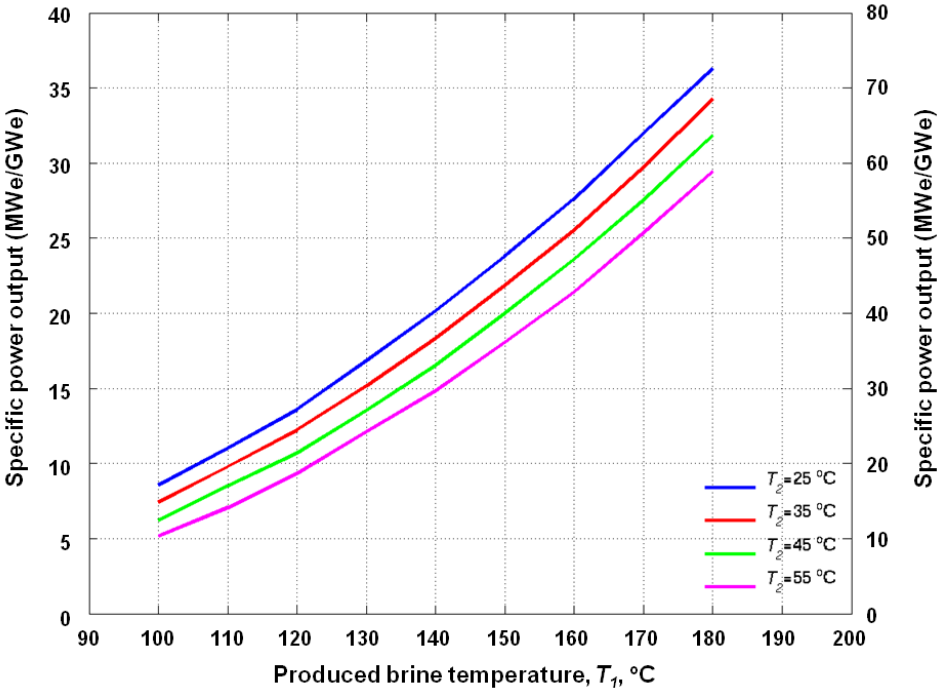

Fig. 4. Specific geothermal power output per GWe of pulverized-coal-fired power generation, when the net extracted volume of brine is equal to the injected CO_2 volume and none of the residual brine is reinjected into the same formation (left y axis). If the ratio of treated brine (produced fresh water) to extracted brine is 0.5 and the residual brine is reinjected into the same formation, the y axis is multiplied by two (right y axis). This plot was obtained by taking Figure 7.3 of MIT (2006), multiplying by 380 (or 760) kg/s, and dividing by 1000 KWe/MWe.

2. Objectives and Methodology

From a CO_2-storage perspective, the key objective for ACRM is for brine production to relieve pressure buildup driven by CO_2 injection. Another objective is to reduce the operational costs of CO_2 storage, which includes the total number of wells and the costs of CO_2 compression and brine pumping (Buscheck et al., 2011c). The operational challenge for ACRM is that pressure relief increases with decreasing spacing between CO_2 injectors and brine producers, while CO_2-breakthrough time decreases. There is a key tradeoff between achieving sufficient pressure relief and delaying CO_2 breakthrough. There are several operational strategies that can better achieve

this trade-off. One strategy is to successively produce brine from a series of producers that are progressively spaced farther from the CO_2 injector (Buscheck et al., 2011a). A second strategy involves horizontal injection and production wells (Buscheck et al., 2011c). A third strategy is the use of "smart wells" (Alhuthali et al., 2007), with down-hole sensors and independently-controlled production and injection intervals to extend the useful lifetime of brine producers.

We begin by investigating the first strategy of producing brine from successively increasing distances from the CO_2 injection well, applied to vertical injectors and producers, and then investigate the second strategy, for horizontal injector/producer-well pairs. We defer consideration of the third strategy (smart wells) and operational costs to future studies. For the vertical-well study, we apply the conceptual model used in earlier studies of saline-formation CO_2 storage (Buscheck et al., 2011a; Zhou et al., 2008), which considered homogeneous formations. For the horizontal-well study, we also considered various storage thickness, dipping and level formations, various caprock thicknesses, and heterogeneous permeability distributions.

In this study we use the NUFT code, developed at Lawrence Livermore National Laboratory for multi-phase multi-component heat and mass flow and reactive transport in unsaturated and saturated porous media (Nitao, 1998; Buscheck et al., 2003; Carroll et al., 2009). The two-phase flow of CO_2 and water was simulated with the density of supercritical-CO_2 determined by the correlation of Span and Wagner (1996). Because the focus of our study is the tradeoff between adequate pressure interference between CO_2 injectors and brine producers and delaying CO_2 breakthrough at brine producers, we assumed isothermal conditions. As long as the breakthrough of injected fluids has not occurred, only native brine will be produced, thus assuring production temperatures will remain at the ambient formation temperature.

A 3-D model is used to analyze vertical wells for a double-ring 9-spot pattern (Fig. 5), with the outer ring of 4 producers rotated 45^o with respect to the inner ring. The 3-D model represents a 250-m-thick storage formation, as modeled by Zhou et al. (2008) and Buscheck et al. (2011a), with the top of the storage formation 1200 m below the water table and bounded by 60-m-thick seal units. The outer boundaries have a no-flow condition to represent a semi-closed system for a 1256-km^2 storage formation. The lower boundary, 1800 m below the water table, has a no flow condition. The upper 1140 m and lower 290 m of the model, called the overburden and underburden, have the same hydrologic properties as the CO_2 storage formation. Hydrologic properties of the storage formation and seal units (Table 1) are similar to previous studies (Zhou et al., 2008; Buscheck et al., 2011a, 2011b, 2011c). CO_2 is injected in a 50-m × 50-m zone in center of the well pattern, in the lower half of the storage formation. Brine is produced in the lower half of the storage formation from 100-m × 100-m zones, and a volumetric balance is always maintained between produced brine and injected CO_2 (extraction ratio = 1). The vertical-well study only considered homogeneous permeability in the storage formation.

For the horizontal-well study, 2-D cross-sectional models were used, with one representing a level storage formation (dip angle of 0^o) and the other of a storage formation with a 10 percent slope (dip angle of 5.7^o). The models represent a semi-closed reservoir system that is 40, 400, and 4000 km in the lateral direction (orthogonal to the well axes) and 4 km in the axial direction, which is parallel to the well axes, with no-flow boundaries at the basement of the storage formation and at the lateral and axial boundaries. As with the 3-D model, this is representative of

a semi-closed system. Storage-formation areas of 160, 1600 and 16000 km^2 are included to investigate the influence of basin size. Storage formation thicknesses of 200 and 400 m are considered, underlain by an impermeable basement and overlain by a caprock with thicknesses of 50, 100, 200, and 400 m. For the model of a level formation, the basement is 1800 m below the water table. For the model of a dipping formation, the basement is 1800 to 4800 m below the water table.

Hydrologic property values (Table 1) are the same as those used in the vertical-well study, with the exception of the consideration of heterogeneous cases with 40-m-thick layers of alternating high and low permeability. Permeability contrasts of 10 and 100 are considered. The CO_2 injection well is located at the lowermost 20 m of the storage formation. The brine-production well is also located at the lowermost 20 m of the storage formation, either 5, 10, 15, or 20 km from the injection well. For the dipping case, the brine producer is located downdip of the CO_2 injector. CO_2 injection rates of 0.475, 0.95, 1.9, 3.8, and 7.6 million tons/year for injection periods of 30 to 100 years are considered. The 2-D model distributes the injection rate uniformly over an axial distance of 4 km.

Table 1. Summary of hydrologic properties used in this study (Buscheck et al., 2011c). The heterogeneous cases are for two different permeability contrasts.

Property		Storage formation	Caprock seal
Horizontal and vertical permeability (m^2)	Homogenous	10^{-13}	10^{-18}
	Heterogeneous 10:1	10^{-13} & 10^{-14}	10^{-18}
	Heterogeneous 100:1	10^{-13} & 10^{-15}	10^{-18}
Pore compressibility (Pa^{-1})		4.5×10^{-10}	4.5×10^{-10}
Porosity		0.12	0.12
van Genuchten (1980) *m*		0.46	0.46
van Genuchten α (Pa^{-1})		5.1×10^{-5}	5.1×10^{-5}
Residual CO_2 saturation		0.05	0.05
Residual water saturation		0.30	0.30

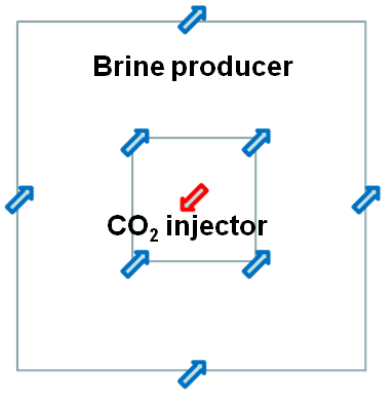

Fig. 5. Plan view of the conceptual model used in the 3-D model used in the vertical-well study, showing the double-ring 9-spot well pattern. The storage-formation area is 1257 km^2.

3. Results of the Vertical-Well Study

We start by contrasting two approaches to pressure management, one with brine production and the other entirely relying on adjusting the CO_2 injection rate. We apply a double-ring 9-spot pattern (Fig. 5) with an inner ring of 4 brine producers 5 km from the CO_2 injector and an outer ring of 4 producers 10 km from the CO_2 injector. The outer ring of producers is rotated by 45 degrees relative to the inner ring (Fig. 1b) to "pull" on the CO_2 plume from different directions to manipulate it into a cylindrical shape. The CO_2 injection rate is 3.8 million tons/year for 60 years and a volumetric balance is maintained between injected CO_2 and produced brine. Brine production occurs entirely from the inner 4 producers during the first 10 years; during the next 5 years, brine production is gradually shifted to the outer 4 producers, while maintaining the same total brine production rate.

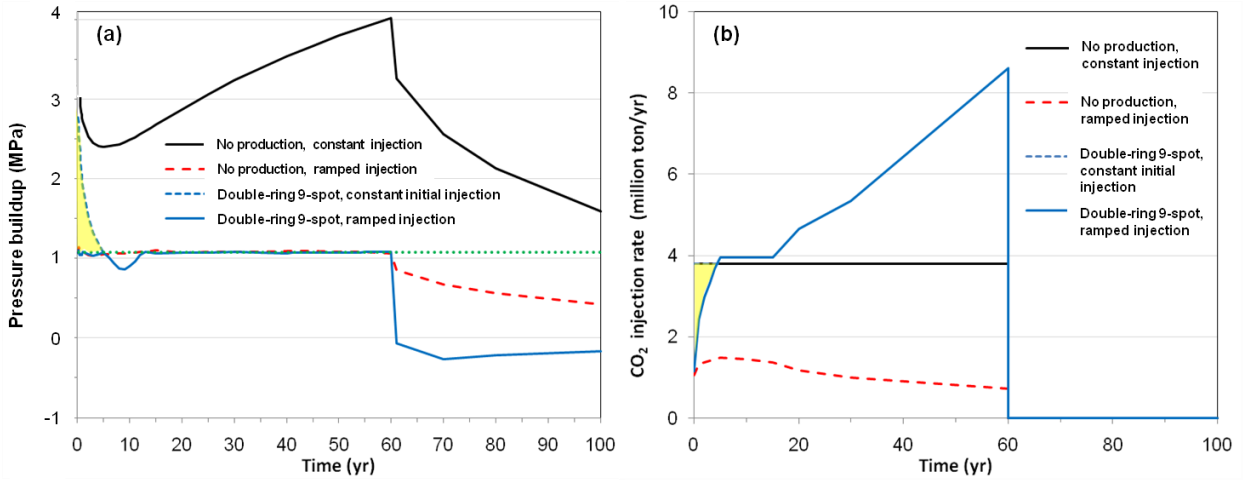

Fig. 6. Pressure buildup at the CO_2 injector (a) and CO_2 injection rate (b) are plotted for two "no-production" cases and two "double-ring 9-spot" cases, all with 60 years of injection. The no-production cases include "constant injection" with a CO_2 injection rate of 3.8 million tons/year and "ramped injection" with injection rate reduced just enough to keep pressure buildup below a specified value (dotted green curve). The double-ring 9-spot cases only differ by virtue of the initial CO_2 injection rates, as depicted by the yellow area in (b), with "constant initial injection" having an initial rate of 3.8 million tons/year and "ramped injection" having the initial rate reduced just enough to keep pressure buildup below the "target" value. The yellow area in (a) shows the influence that initial CO_2 injection rate reduction has on pressure buildup.

The objective of this pressure management example is to not exceed a target value of peak pressure buildup (ΔP_{peak}), which is the pressure in excess of ambient. We chose a ΔP_{peak} target of 1.08 MPa for reasons explained in Buscheck et al. (2011c). In general, a target value of ΔP_{peak} would be related to mitigating risks, such as those related to fracture initiation (Morris et al., 2011) or fault activation (Rutqvist et al., 2007). The no-production case with a constant CO_2 injection rate of 3.8 million tons/year (Fig. 6b) results in an initial ΔP_{peak} of 2.95 MPa and an ultimate ΔP_{peak} of 4.06 MPa, at the end of injection (Fig. 6a). For the double-ring 9-spot with a constant initial CO_2 injection rate of 3.8 million tons/year, ΔP is initially 2.95 MPa, declining to 1.07 MPa at 5 years. To keep ΔP just at the target value, CO_2 injection rate is reduced to an initial value of 1.2 million tons/year, ramped up to 4.0 million tons/year at 5 years, and held

constant until 15 years (Fig. 6b). At 15 years, brine production has completely shifted to the outer 4 producers at 10 km. Because pressure relief increases with time, it is possible to continuously ramp up CO_2 injection rate from 4.0 to 8.6 million tons/year for duration of the injection period (Fig. 6b) and remain close to the ΔP target (Fig. 6a). To keep ΔP at the target for the no-production case, CO_2 injection must be reduced to an initial rate of 1.1 million tons/year, slowly increased to 1.5 million tons/year at 5 years, then gradually reduced to 0.7 million tons/year at 60 years.

A way to quantify the pressure-relieving benefit of brine production is the injectivity ratio, determined by dividing CO_2 injection rate for the brine-production case by CO_2 injection rate for the no-production case for the same value of ΔP (Buscheck et al., 2011c). Thus, injectivity ratio varies continuously with time. For this example, the injectivity ratio starts at a value of 1.1, increasing to 2.7, 5.4, and 12.2 at 5, 30, and 60 years, respectively. For the 60-year injection period, brine production enables a 5.5-fold increase in stored CO_2, compared to the no-production case. It is worth noting that CO_2 breakthrough never occurred at the inner ring of producers at 5 km, while for the outer 4 producers, CO_2 breakthrough occurred at 50 years. Therefore, for this example, production temperatures would remain at the ambient formation temperature for at least 50 years. Considering the very long residence time for the CO_2 en route to the brine producers, it is likely that the CO_2 would have been nearly heated to ambient formation temperatures prior to breakthrough. Therefore, thermal drawdown would probably be relatively minor during the final 10 years of the injection period, enabling sustainable geothermal energy production.

4. Results of the Horizontal-Well Study

We consider a 400-m-thick CO_2-storage formation, with an area of 160 km^2, overlain by a 400-m-thick caprock, and with a 10% dip. The brine producer is located 10 km downdip from the CO_2 injector. Supercritical CO_2 flows preferentially through high-permeability layers (Figure 7), while diffusion of aqueous-phase CO_2 distributes CO_2 into the low-permeability layers (Buscheck et al., 2011c). Homogeneous permeability allows buoyancy to drive CO_2 updip for the no-production case (Fig. 7a). Brine production 10 km downdip of the CO_2 injector negates the influence of buoyancy (Fig. 7b), pulling the CO_2 plume down to the brine producer, where breakthrough occurs at 46 years. Layered heterogeneous permeability impedes buoyancy-driven migration of CO_2 (Fig. 7c) for the no-production case. When the permeability contrast is increased, layered heterogeneity in the storage formation more strongly impedes the buoyancy-driven migration of CO_2 (Fig. 7e). For the case with brine production, layered heterogeneous permeability causes the CO_2 plume to be more evenly distributed vertically in the storage formation, which delays the arrival of CO_2 at the brine producer, increasing breakthrough time to 50 years (Fig. 7d). When the permeability contrast is increased, layered heterogeneity much more evenly distributes CO_2 vertically in the storage formation, which further delays the arrival of the CO_2 at the brine producer, increasing breakthrough time to 75 years (Figs. 7f). These CO_2 breakthrough times indicate geothermal production can be maintained at ambient formation temperatures for an economically attractive timeframe.

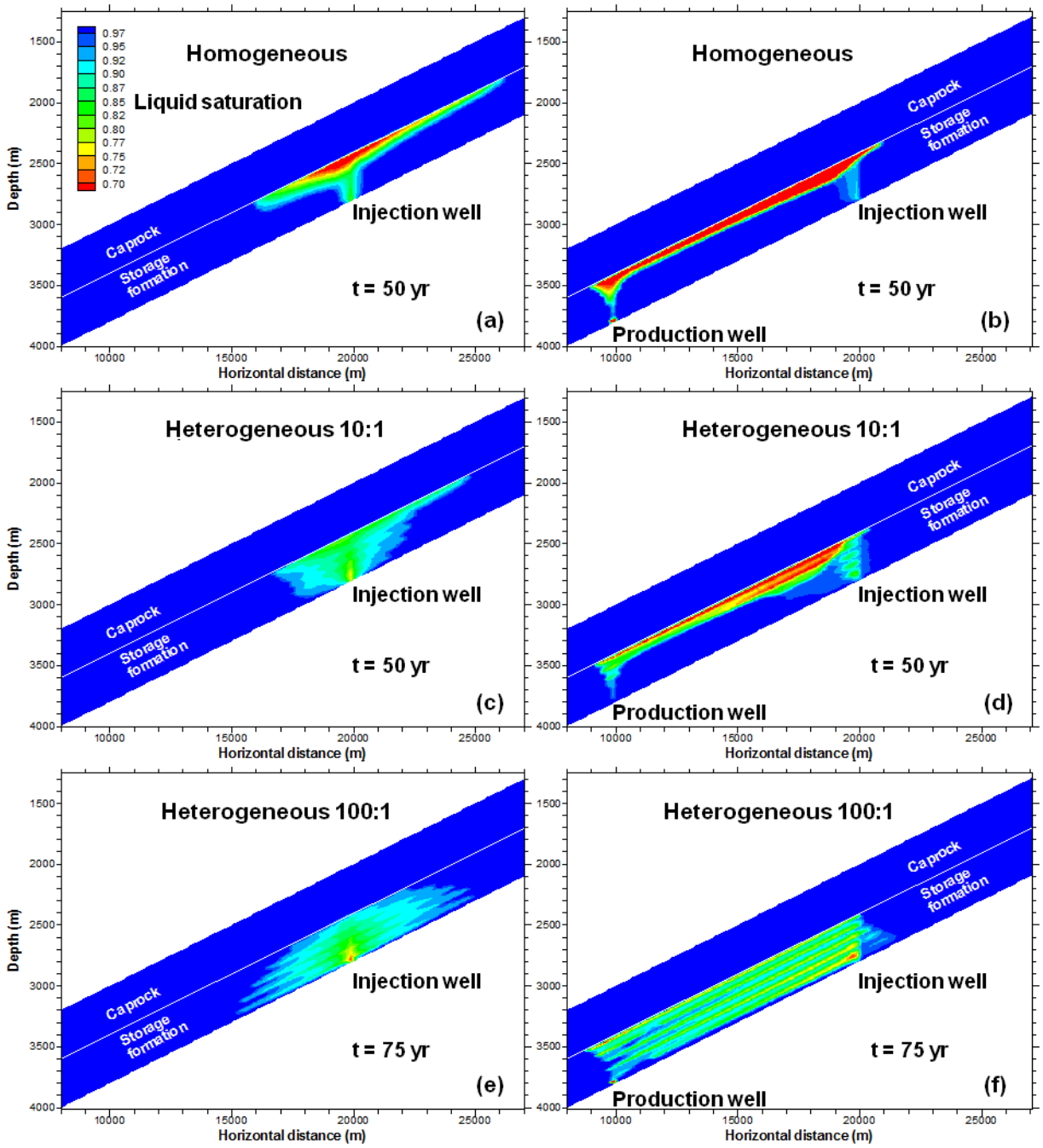

Fig. 7. Liquid saturation contours show CO_2-plume migration driven by CO_2 injection from a horizontal well for no brine production (a,c,e), and for brine produced in a horizontal well 10 km downdip from the injection well (b,d,f). Storage-formation-permeability cases are homogeneous (a, b), layered heterogeneity with a permeability contrast of 10 (c,d), and layered heterogeneity with permeability contrast of 100 (e,f). The heterogeneous cases have alternating 40-m-thick layers of high and low permeability. The horizontal injectors and producers are located in the lower 20 m of the storage formation. The vertical scale is exaggerated by a factor of 5.

We now consider the relationship between ΔP_{peak}, injectivity, and CO_2 breakthrough time. Fig. 8a shows ΔP_{peak} increasing with CO_2 injection rate and well spacing between the producer/injector pair. The pressure-relieving effect of brine production is seen as a reduction in slope of ΔP_{peak} versus CO_2 injection rate (Q_{inj}) curve. Because pressure relief increases with decreasing well spacing, the slope is reduced with decreasing well spacing. Heterogeneity has a modest influence on ΔP_{peak} for the no-production case, while for cases with brine production the influence on ΔP_{peak} is much stronger. For the heterogeneous case, effective permeability in the horizontal direction is reduced by nearly 50 percent. Accordingly, this influence is seen to be nearly equivalent to doubling the well spacing.

Injectivity ratio quantifies the pressure-relieving benefit of brine production. For the horizontal-well study, we define injectivity ratio with respect to the ΔP_{peak}, rather than ΔP as a function of time. Thus, injectivity ratio is the CO_2 injection rate for the brine-production (ACRM) case divided by the CO_2 injection rate for the no-production case for the same value of ΔP_{peak}. For the horizontal-well study, the injectivity ratio pertains to the injection period as a whole. Because we assume equal perforated lengths of the CO_2 injectors and brine producers, an injectivity ratio greater than 2 indicates potential savings in well-drilling costs.

Because pressure relief decreases with increasing well spacing, injectivity ratio also decreases with increasing well spacing (Fig. 8b). Injectivity ratio is insensitive to CO_2 injection rate. Because ΔP_{peak} is more sensitive to heterogeneity for the brine-production cases than for the no-production cases, injectivity ratio is less for the heterogeneous cases. If the average horizontal permeability had been kept fixed between the homogeneous and heterogeneous cases, it is likely that the injectivity ratio would not have been substantially reduced in the heterogeneous case. Therefore, what is being exhibited is that injectivity ratio decreases with decreasing permeability, not by virtue of the existence of heterogeneity.

CO_2 breakthrough time increases with well spacing (Fig. 9a). For a level formation (0% dip), heterogeneity causes preferential (channeled) flow of CO_2 that reduces CO_2 breakthrough time. For 10-km well spacing and a CO_2 injection rate of 3.8 million tons/year, CO_2 breakthrough occurs at 45 and 30 years for the homogeneous and heterogeneous cases, respectively, while for an injection rate of 7.6 million tons/year, CO_2 breakthrough occurs at 19 and 18 years. Heterogeneity can have the opposite influence on CO_2 breakthrough time, depending on formation dip and where brine producers are located, relative to the CO_2 injector. Compared to level placement in a level storage formation, placing a brine producer downdip of the CO_2 injector can substantially increase CO_2 breakthrough time, particularly for layered heterogeneous permeability (Fig. 9b). Therefore, it is possible to take advantage of the influence of buoyancy on CO_2-breakthrough time. The beneficial influence of buoyancy on delaying CO_2 breakthrough increases with dip angle and with permeability contrast (compare Figs.7d and 7f).

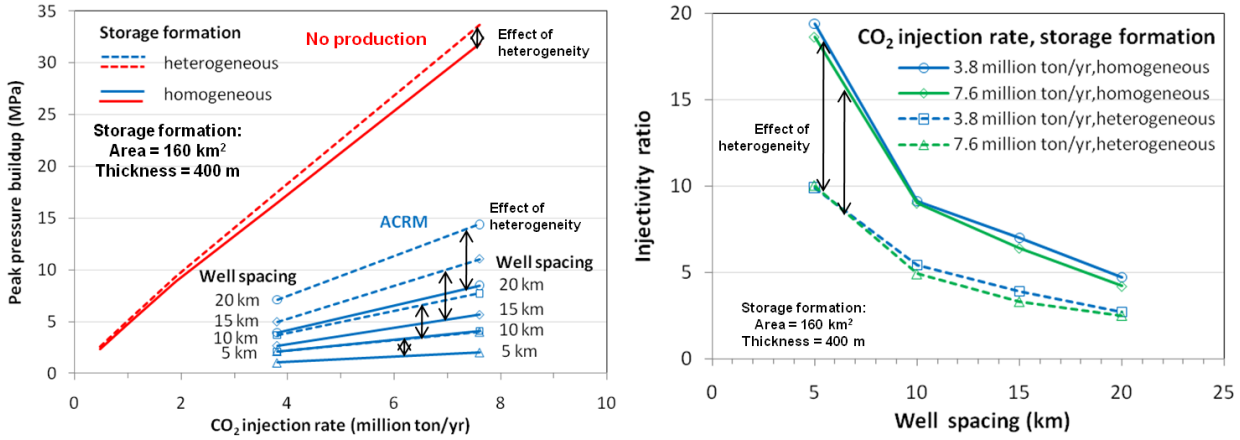

Fig. 8. (a) CO_2 breakthrough time is plotted versus well spacing between horizontal CO_2 injectors and brine producers for the set of ACRM cases plotted in Fig. 7b. (b) The influence of formation dip on CO_2 breakthrough time is shown for a CO_2-injection rate of 3.8 million tons/year, by comparing level cases (0% dip) with cases having a 10% dip. Heterogeneous cases have alternating 40-m-thick layers of high and low permeability, with a permeability contrast of 10. The storage formation is 400 m thick, overlain by a 400-m-thick caprock, the injection period is 30 years, and storage-formation area is 160 km^2.

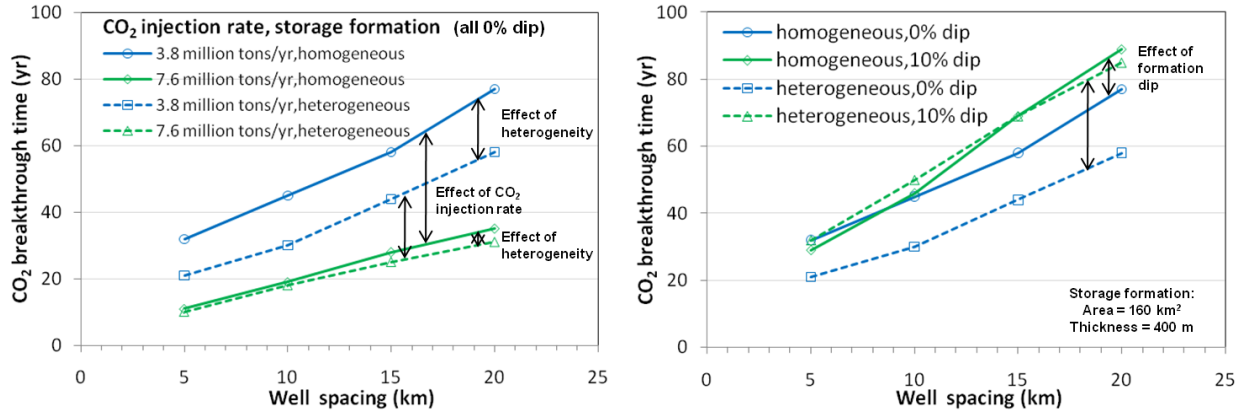

Fig. 9. (a) CO_2 breakthrough time is plotted versus well spacing between horizontal CO_2 injectors and brine producers for the set of ACRM cases plotted in Fig. 8b. (b) The influence of formation dip on CO_2 breakthrough time is shown for a CO_2-injection rate of 3.8 million tons/year. Heterogeneous cases have alternating 40-m-thick layers of high and low permeability, with a permeability contrast of 10. The storage formation is 400 m thick with an area of 160 km^2 and is overlain by a 400-m-thick caprock.

Reducing storage formation thickness by a factor of 2 has a relatively small effect on injectivity ratio (Fig. 10a), while having a stronger influence on CO_2 breakthrough time (Fig. 10b). Reducing the storage-formation thickness by a factor of 2 reduces CO_2 breakthrough time by slightly less than a factor of 2 for the heterogeneous case and by a factor of slightly greater than 2 for the homogeneous case. Increasing storage-formation area by a factor of 10 (or 100) reduces ΔP_{peak} around the CO_2 injector by 30 to 40 percent (increasing with CO_2 injection rate) for the no-production case (Fig. 11a). This is expected because there is considerably greater area for pressure buildup to be dissipated through the caprock and greater storage-formation volume over which fluid compression can occur. For cases with brine production, ΔP_{peak} is insensitive to

storage-formation area for well spacings of 5, 10, and 15 km and only slightly sensitive for 20-km well spacing (Fig. 11a). Accordingly, increasing the storage-formation area by a factor of 10 (or 100) reduces injectivity ratio by about 30 to 40 percent (increasing with CO_2 injection rate) (Fig. 11b). Injectivity ratios are still much greater than 2 for well spacings of 10 km or less and are greater than 2 for well spacings of 15 and 20 km. Because storage-formation area does not influence CO_2 breakthrough time, it was not necessary to include plots of that influence. For caprock thicknesses of 50 to 400 m, we found that ΔP_{peak}, injectivity ratio, and CO_2 breakthrough time are all insensitive to caprock thickness.

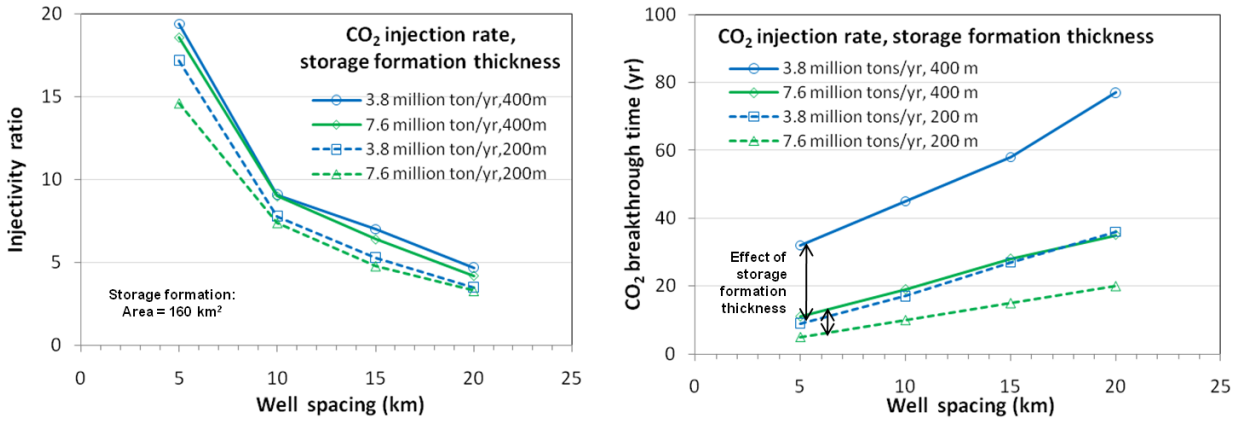

Fig. 10. (a) Injectivity ratio and (b) CO_2 breakthrough time are plotted versus well spacing between horizontal injector/producer pairs for storage-formation thicknesses of 200 and 400 m. The storage formation has homogeneous permeability, the caprock is 400 m thick, the injection period is 30 years, and storage-formation area is 160 km^2.

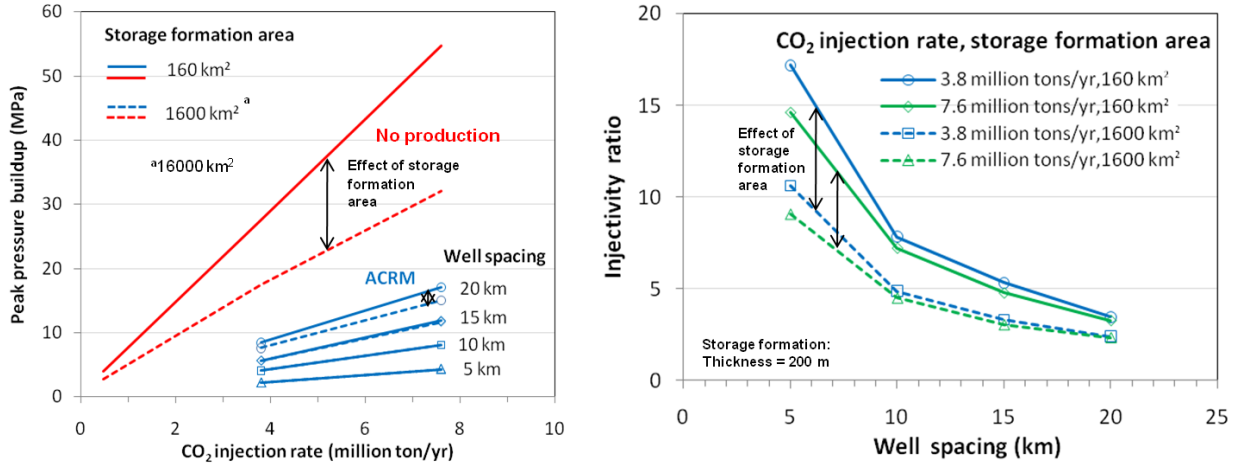

Fig. 11. (a) Peak pressure buildup versus CO_2 injection rate is plotted for horizontal-well cases with no brine production and with brine produced from horizontal wells 5, 10, 15, and 20 km from the injector for storage-formation areas of 160, 1600, and 16000 km^2. The storage formation is level, 200 m thick, with homogeneous permeability, and overlain by a 400-m thick caprock. (b) For the same set of cases, injectivity ratio is plotted versus well spacing between injector/producer pairs for CO_2-injection rates of 3.8 and 7.6 million tons/year. The injection period is 30 years. The curves for storage-formation areas of 1600 and 16000 km^2 are the same.

After ΔP_{peak} occurs, the influence of brine production on pressure relief at the CO_2 injector increases with time (Fig. 12). Because ΔP_{peak} occurs relatively early during the injection period, ΔP_{peak} is insensitive to storage-formation area. The strong influence of brine production on pressure relief around the CO_2 injector indicates that, after ΔP_{peak} is attained, it should be possible to continuously ramp up the CO_2 injection rate while remaining just below a target value of ΔP, as was done in the double-ring 9-spot pressure-management example discussed earlier (Fig. 6).

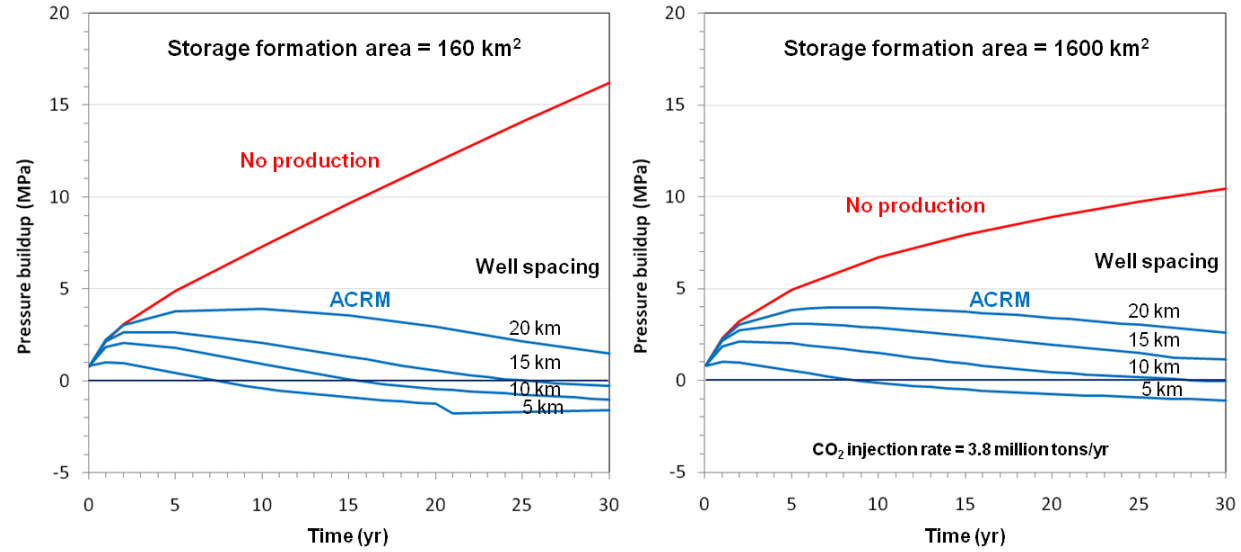

Fig. 12. Pressure buildup history is plotted for horizontal-well cases with no brine production and with brine produced from horizontal wells 5, 10, 15, and 20 km from the CO_2 injector for a storage-formation area of (a) 160 km^2 and (b) 1600 km^2 (also 16000 km^2). The storage formation is level, 400 m thick, with homogeneous permeability, overlain by a 400-m-thick caprock. The injection period is 30 years.

Consideration of Figs. 8, 9, and 12 indicates the potential benefits of successively producing brine from more than one horizontal well. For a 400-m-thick formation and a CO_2 injection rate of 3.8 million tons/year, brine production from a producer 5 km from the CO_2 injector could increase injectivity by a factor of 10 (Fig. 8b), which could continue for at least 20 years, corresponding to the earliest CO_2 breakthrough time (Fig. 9b). Brine production could be gradually shifted to a producer 20 km from the CO_2 injector, providing the same degree of pressure relief that was achieved at early time from the producer at 5 km (Fig. 12), while delaying CO_2 breakthrough to 60 years or more (Fig. 9b), thereby sustaining geothermal power production for a highly attractive economic timeframe.

5. Conclusions

We investigate a synergistic approach to producing geothermal energy and sequestering CO_2 at low cost and risk by integrating geothermal production with CO_2 capture and storage (CCS) in deep, saline, sedimentary formations, where a significant portion of the U.S. geothermal resource resides, and where there is also a large need for CCS implementation. For industrial-scale, saline-formation CCS, pressure buildup can be a limiting factor in storage capacity and security, while for geothermal energy production the limiting factor can be pressure depletion. These two systems can be combined in a complementary fashion, with CO_2 injection providing pressure

support to maintain productivity of geothermal wells, and geothermal brine production providing pressure relief and improved injectivity for CO_2 injectors. The key tradeoff for our approach is that pressure relief increases with decreasing spacing between injectors and producers, while CO_2 breakthrough time decreases. We considered two operational strategies that can better achieve this tradeoff, with the first strategy involving successively producing brine from producers spaced progressively farther from the CO_2 injector, and the second involving the use of horizontal wells. We found that a vertical-well, double-ring 9-spot pattern of brine producers around a CO_2 injector can achieve a large increase in injectivity, while delaying CO_2 breakthrough for greater than 30 years. For a horizontal injector/producer pair, we find that even a larger increase in injectivity is possible, while delaying CO_2 breakthrough for much greater than 30 years. Combining these strategies, together with smart-well technology, can result in even greater benefits. Our results indicate that integrating geothermal with CCS in sedimentary formations has the potential of providing sustainable, low-cost geothermal power, while increasing CO_2 storage capacity and security.

Acknowledgements
This work performed under the auspices of the U.S. Department of Energy by Lawrence Livermore National Laboratory under Contract DE-AC52-07NA27344.

References

Aines, R.D., Wolery, T.J., Bourcier, W.L., Wolfe, T, and Haussmann, C.W., 2011. Fresh water generation from aquifer-pressured carbon storage: Feasibility of treating saline formatiom waters, *Energy Procedia*, 4, 2269–2276.

Alhuthali, A.H., Oyerinde, D., and Datta-Gupta, A., 2007. Optimal waterflood management using rate control, SPE Reservoir Evaluation & Engineering, 10 (4): 539-551, October. DOI: 10.2118/102478-PA.

Birkholzer, J.T. and Zhou, Q., 2009. Basin-scale hydrogeologic impacts of CO_2 storage: Capacity and regulatory implications, *International Journal of Greenhouse Gas Control* 3, 745–756.

Bourcier, W.L., Burton, E., and Newmark, R., 2007. New materials and separations science for sustainable water, First Western Forum on Energy and Water Sustainability, University of California, Santa Barbara, March 22-23.

Bourcier W.L., Wolery, T.J., Wolfe, T., Haussmann, C., Buscheck, T.A., and Aines, R.D., 2011. A preliminary cost and engineering estimate for desalinating produced formation water associated with carbon dioxide capture and storage, *International Journal of Greenhouse Gas Control*, submitted.

Buscheck, T.A., Glascoe, L.G., Lee, K.H., Gansemer, J., Sun, Y., and Mansoor, K., 2003. Validation of the multiscale thermohydrologic model used for analysis of a proposed repository at Yucca Mountain, *Journal of Contaminant Hydrology*, 62 (3), 421–440.

Buscheck, T.A, Sun, Y., Hao, Y., Wolery, T. J., Bourcier, W.L., Tompson, A.F.B., Jones, E.D., Friedmann, S.J., and Aines, R.D., 2011a. Combining brine extraction, desalination, and residual-brine reinjection with CO_2 storage in saline formations: Implications for pressure management, capacity, and risk mitigation, *Energy Procedia*, 4, 4283–4290.

Buscheck, T.A., 2010. Active management of integrated geothermal-CO_2-storage reservoirs in sedimentary formations: An approach to improve energy recovery and mitigate risk, Proposal in response to DE-FOA-0000336: Energy Production with Innovative Methods of Geothermal Heat Recovery, LLNL-PROP-463758.

Buscheck, T.A., Sun, Y., Wolery, T.J., Court, B., Celia, M.A., Friedmann, S.J., and Aines, R.D., 2011b. Active CO_2 reservoir management in saline formations: Utilizing synergistic opportunities to increase storage capacity, reduce cost, and mitigate risk, presentation at the SPE International Workshop on Carbon Capture, Utilization, and Storage (CCUS): Environment, Energy Security, and Opportunities for the Middle East, 7–9 March, Abu Dhabi, UAE.

Buscheck, T.A., Sun, Y., Chen, M., Hao, Y., Wolery, T.J., Bourcier, W.L., Court, B., Celia, M.A., Friedmann, S.J., and Aines, R.D., 2011c. Active CO_2 reservoir management for carbon storage: analysis of operational strategies to relieve pressure buildup and improve injectivity, *International Journal of Greenhouse Gas Control*, doi:10.1016/j.ijggc.2011.11.007.

Carroll, S.A., Hao, Y., and Aines, R.D., 2009. Geochemical detection of carbon dioxide in dilute aquifers. Geochemical Transactions 10, 4.

Court, B., Celia, M.A., Nordbotten, J.M., and Elliot, T.R., 2011a. Active and integrated management of water resources throughout CO_2 capture and sequestration operations, *Energy Procedia*, 4, 4221–4229.

Court, B., Bandilla, K., Celia, M.A., Buscheck, T.A., Nordbotten, J., Dobossy, M., and Jansen, A., 2011b. Initial evaluation of advantageous synergies associated with simultaneous brine production and CO_2 geological sequestration, *International Journal of Greenhouse Gas Control*, in review.

Harto, C.B. and Veil, J.A., 2011. Management of water extracted from carbon sequestration projects. Argonne National Laboratory, ANL/EVS/R-11/1.

MIT, 2006. The Future of Geothermal Energy: Impact of Enhanced Geothermal Energy Systems (EGS) in the United States in the 21st Century.

Morris J.P., Detwiler, R.L., Friedmann, S.J., Vorobiev, O.Y., and Hao, Y., 2011. The large-scale geomechanical and hydrological effects of multiple CO_2 injection sites on formation stability, *International Journal of Greenhouse Gas Control*, 5, 69-74.

Neal, P.R, Cinar, Y., and Allinson, W.G., 2011. The economics of pressure-relief with CO_2 injection, *Energy Procedia*, 4, 4215–4220.

Nitao, J.J., 1998. Reference manual for the NUFT flow and transport code, version 3.0, Lawrence Livermore National Laboratory, UCRL-MA-130651-REV-1.

Rutqvist, J., Birkholzer, J., Cappa, F., Tsang, C.-F., 2007. Estimating maximum sustainable injection pressure during geological sequestration of CO_2 using coupled fluid flow and geomechanical fault-slip analysis. Energy Conversion and Management 48, 1798–1807.

Span, R. and Wagner, W., 1996. A new equation of state for carbon dioxide covering the fluid region from the triple-point temperature to 1100K at pressures up to 800 MPa. *Journal of Physical and Chemical Reference Data*, 25, 1509–1596.

Surdam, R.C., Jiao, Z., Stauffer, P., and Miller, T., 2009. An integrated strategy for carbon management combining geological CO_2 sequestration, displaced fluid production, and water treatment, Wyoming State Geological Survey, Challenges in Geologic Resource Development No. 8.

van Genuchten, M.T., 1980. A closed form equation for predicting the hydraulic conductivity of unsaturated soils. *Soil Science Society of America Journal*, 44: 892-898.

Zhou, Q., Birkholzer, J.T., Tsang C-F., and Rutqvist, J. A., 2008.A method for quick assessment of CO_2 storage capacity in closed and semi-closed saline formations. *International Journal of Greenhouse Gas Control*, 2, 626-639.